Tuning InAs/GaAs quantum dot properties under Stranski-Krastanov growth mode for 1.3 μm applications

Tuning InAs/GaAs quantum dot properties under Stranski-Krastanov growth mode for 1.3 μm applications

J. X. Chen, A. Markus, A. Fiore,[a] U. Oesterle, R. P. Stanley, J. F. Carlin, R. Houdré, and M. Ilegems
Institute of Quantum Photonics and Electronics, Ecole Polytechnique Fédérale de Lausanne, CH-1015 Lausanne, Switzerland

L. Lazzarini and L. Nasi
CNR-IMEM Institute, Parco Area delle Scienze, Parma, Italy

M. T. Todaro, E. Piscopiello, and R. Cingolani
Unità INFM, Dipartimento Ingegneria dell'Innovazione, Università di Lecce, Italy

M. Catalano
INE-CNR, Via Arnesano, 73100 Lecce, Italy

J. Katcki and J. Ratajczak
Institute of Electron Technology, Aleja Lotnikow 32/46,02 668 Warszawa, Poland

(Received 5 November 2001; accepted for publication 13 March 2002)

In this paper, we present a systematic study of the effect of growth parameters on the structural and optical properties of InAs quantum dot (QD) grown under Stranski–Krastanov mode by molecular beam epitaxy. The dot density is significantly reduced from 1.9×10^{10} to 0.6×10^{10} cm^{-2} as the growth rate decreases from 0.075 to 0.019 ML/s, while the island size becomes larger. Correspondingly, the emission wavelength shifts to the longer side. By increasing the indium fraction in the InGaAs capping layer, the emission wavelength increases further. At indium fraction of 0.3, a ground state transition wavelength as long as 1.4 μm with the excited state transition wavelength of around 1.3 μm has been achieved in our dots. The optical properties of QDs with a ground state transition wavelength of 1.3 μm but with different growth techniques were compared. The QDs grown with higher rate and embedded by InGaAs have a higher intensity saturation level from excitation dependent photoluminescence measurements and a smaller intensity decrease from temperature dependent measurements. Finally, single mirror light emitting diodes with a QD embedded in InGaAs have been fabricated. The quantum efficiency at room temperature is 1.3%, corresponding to a radiative efficiency of 21.5%. © *2002 American Institute of Physics.*
[DOI: 10.1063/1.1476069]

I. INTRODUCTION

Semiconductor quantum dots (QDs) have attracted considerable interest during recent years. These nanostructures provide a three dimensional (3D) confinement potential for the carriers and consequently have a discrete energy spectrum with δ-like densities of states and ultranarrow gain spectrum.[1–3] They have already been utilized in electronic and optoelectronic devices, such as semiconductor lasers,[4–7] light emitting diodes (LEDs),[8–10] single electron transistors,[11] and more recently single photon emitters.[12,13] QDs may also allow one to extend the emission wavelength of GaAs-based devices to the telecommunication wavelength range of 1.3~1.55 μm. This would be particularly interesting, owing to the essential advantages of GaAs-based semiconductor lasers over InP-based ones, such as lower temperature sensitivity, more mature material, and device process technology, and in particular, the large index difference between GaAs and AlAs, which allows the fabrication of high performance vertical cavity surface emitting lasers (VCSELs).

Under Stranski–Krastanov (SK) growth mode, the formation of quantum dots is driven by the strain during epitaxy growth of In(Ga)As on a GaAs substrate as the deposited layer exceeds a critical thickness. Correspondingly the growth mode switches from a two dimensional (2D) growth to a three dimensional growth. The strain is relieved elastically without introduction of crystal defects. The dot size, areal density, and optical properties depend on the growth parameters, such as growth temperature, growth rate, and group III over V ratio. The emission wavelength of In(Ga)As QDs can be tuned between 1~1.7 μm by varying the growth conditions, thus covering the important telecommunication wavelength range, even though at present most studies on In(Ga)As QDs concentrate on 1.3 μm. A common technique to extend the emission wavelength to 1.3 μm is to embed the quantum dot in an InGaAs matrix rather than in a GaAs matrix. The red shift of InGaAs embedded QDs is attributed to the increase of the dot height caused by spinoidal activated decomposition and to reduced strain.[14,15] 1.3 μm lasers with extremely low threshold current have been successfully demonstrated for InGaAs capped QDs. Another possible way to obtain 1.3 μm emission wavelength is to make large sized dots by reducing growth rate.[16] This technique has the ad-

[a]Electronic mail: fiore@dpmail.epfl.ch

vantage of a smaller total amount of indium as compared to InGaAs embedded dots.

In this paper, we present a systematic study of the effect of growth rate and InGaAs capping layer on the structural and optical properties of InAs QDs. We demonstrate that the emission wavelength of In(Ga)As QDs can be extended to 1.4 μm. We compare the optical properties of QDs with emission wavelength of 1.3 μm obtained by the two different approaches mentioned above. Finally we report single mirror light emitting diodes (SMLED) with high quantum efficiency.

II. EXPERIMENTS

The growth was conducted on a solid source molecular beam epitaxy system equipped with an As cracker cell. The InAs quantum dots were formed by continuously depositing 2.9 ML InAs on a GaAs (500 nm)/AlAs(20 nm) GaAs(100 nm) buffer layer on Si-doped (100) GaAs substrate and covered either first with InGaAs or directly with GaAs (100 nm)/AlAs (20 nm)/GaAs (10 nm). The growth temperature is 535 °C for the InAs and 620 °C for the other layers. The InAs growth rate was varied from 0.15 to 0.009 ML/s and the 2D→3D growth mode transition was followed by monitoring the change in the *in situ* reflection high energy electron diffraction (RHEED) pattern. The indium flux was calibrated at higher growth rate while the cell temperatures for the lower growth rate were deduced by thermal calculation. The background As_2 pressure was maintained at 5×10^{-7} mbar during the growth of all the layers.

Atomic force microscopy (AFM) measurements were performed on bare quantum dots. In that case, the growth stopped after InAs deposition and the temperature was quickly lowered in order to freeze the islands. Transmission electron microscopy (TEM) was performed on capped quantum dot samples in a JEOL 2000FX microscope. Specimens were prepared in planar and cross-sectional geometry using conventional mechanical polishing down to ~20 μm and then brought to electron transparency by ion milling. For photoluminescence (PL) measurements, the samples were excited with a Ti:sapphire laser ($\lambda = 800$ nm). The signal was spectrally dispersed by a grating monochromator and detected with an uncooled InGaAs photodiode.

III. RESULTS AND DISCUSSION

A. The effect of the growth rate

Three AFM images taken from samples grown at different growth rate of 0.075, 0.037, and 0.019 ML/s are shown in Figs. 1(a), 1(b), and 1(c). The QD density is reduced significantly from 1.9×10^{10} to 1.4×10^{10} cm^{-2} and further to 0.6×10^{10} cm^{-2} as the growth rate decreases, while the island size becomes larger. The total amount of deposited InAs is the same in the three cases as noted previously. It is interesting to point out that the 2D to 3D growth mode transition according to the RHEED pattern occurred at the same amount of deposited InAs layer, approximately 1.8 ML.

Figure 2(a) shows the room temperature PL spectra of QDs grown at different growth rates and 2(b) depicts the corresponding peak wavelength and full width at half maximum (FWHM) of each spectrum. The emission wavelength shifts from 1163 to 1265 nm with a concomitant narrowing of the linewidth from 42 to 32 meV as the growth rate decreases from 0.15 to 0.019 ML/s. The emission wavelength

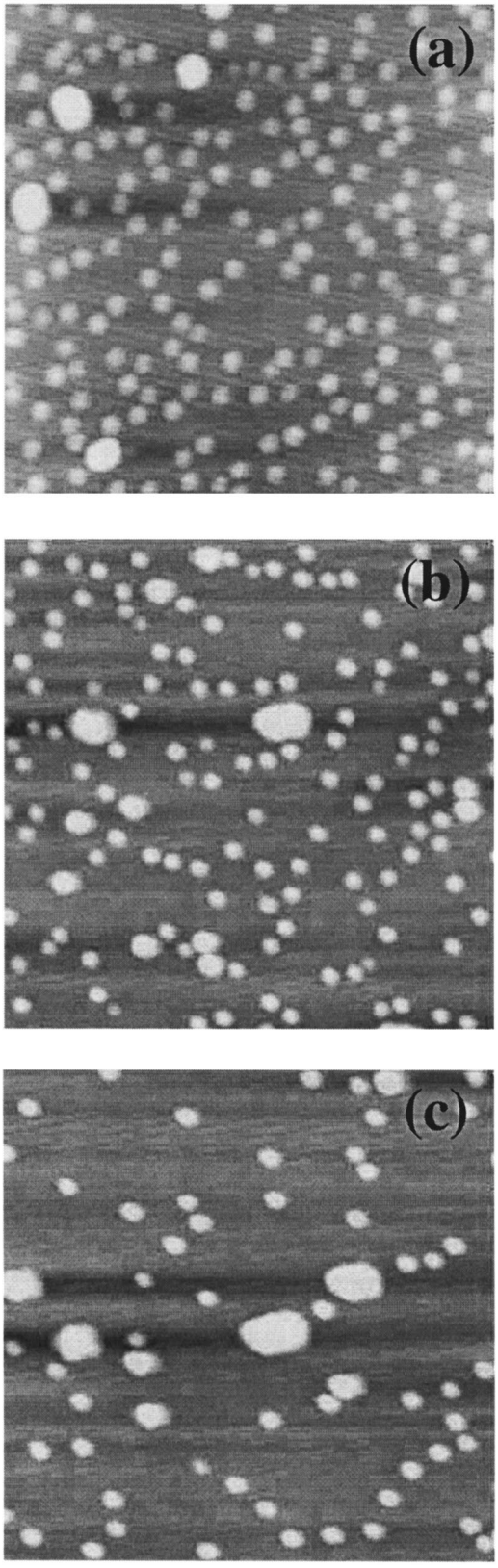

FIG. 1. AFM images of InAs quantum dots grown at different growth rate of 0.075 ML/s (a), 0.037 ML/s (b), and0.019 ML/s (c). The QD densities are 1.9×10^{10}, 1.4×10^{10}, and 0.6×10^{10} cm^{-2}, respectively.

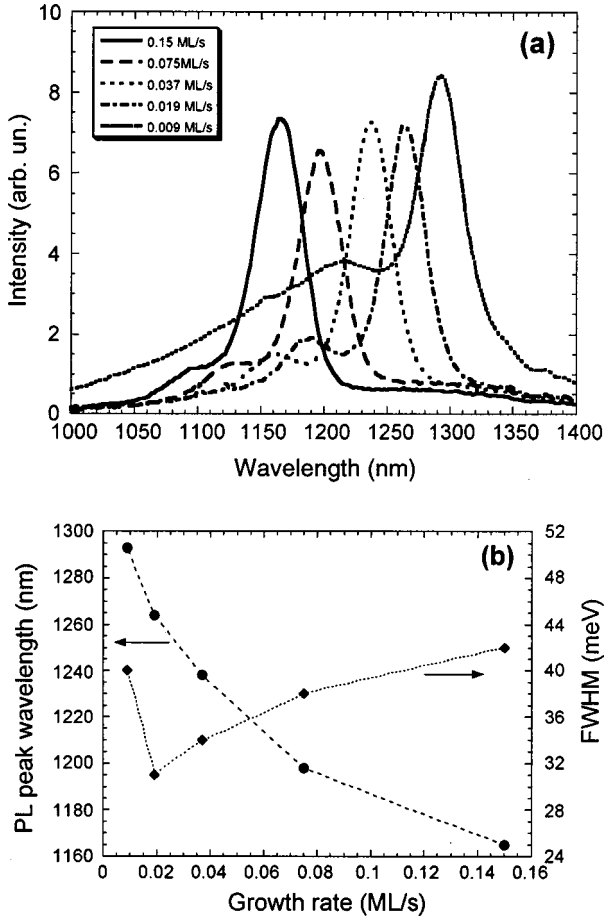

FIG. 2. PL spectra (a) and peak wavelength and FWHM (b) of InAs QDs grown at different grown rates. All samples were grown at substrate temperature of 535 °C, except the sample with 0.009 ML/s growth rate, which was at 520 °C.

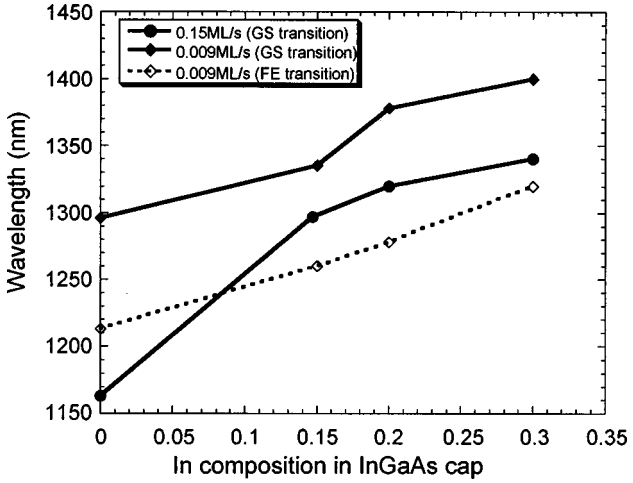

FIG. 3. Emission wavelength of QDs grown at rates of 0.15 and 0.009 ML/s as a function of In fraction in InGaAs capping layer.

reaches 1280 nm at the growth rate of 0.009 ML/s (not shown in the figure) and it further increases to 1300 nm, as shown in Fig. 2 by decreasing the growth temperature from 535 to 520 °C. The narrowing of the FWHM indicates that the island size dispersion was suppressed by reduction of growth rate. The redshift of emission wavelength can be directly linked to the increase in dot size from our AFM observation while scanning tunneling microscopy (STM) studies[16] revealed that the indium fraction in the dot was also dependent on the growth rate, being higher at lower growth rate.

It is very difficult to exactly explain how growth rate affects quantum dot structural properties, while some models can be employed to qualitatively understand the growth dependence of the dot density and size. The mean-field rate equation theory of Dobbs *et al.*[17] was used to reproduce the dependence of the 3D island density on the growth rate and temperature in the metalorganic vapor phase epitaxial growth of InP and GaP stabilized GaAs (001), showing higher island densities at low temperatures and high growth rate. Under the same framework, it is not difficult to understand the dot density reduction at lower growth rate in our experiments. Using energetic calculation, Tersoff[18] predicts higher indium fraction in quantum dot at lower growth temperature, which is qualitatively consistent with our finding that emission wavelength further red-shift as the growth temperature decreases from 535 to 520 °C. Generally speaking, under SK growth mode, the incident atoms diffuse across the reconstructed surface and arrange themselves, starting from the step edges, to form a continuous layer [wetting layer (WL)]. As growth proceeds, 3D islands form to minimize the total energy, which includes surface, interfacial, and elastic strain energies of the epitaxial film. After the formation of the 3D islands, the incident adatoms are preferably incorporated into existing islands since this is energetically favorable. As the growth rate decreases, the adatoms have a higher chance to be incorporated into the existing islands since their diffusion length increases. Thus, the reduction of the growth rate reduces the dot density and increases the island size correspondingly.

B. The effect of InGaAs capping layer

The InGaAs capping layer thickness was fixed at 5 nm while the indium fraction was varied in our experiments. The InAs islands were grown at two different growth rates of 0.15 and 0.009 ML/s. Figure 3 shows the ground state (GS) transition wavelength of QDs at 0.15 ML/s growth rate and the ground transition and first excited state (FE) transition wavelength of QDs at 0.009 ML/s. For the QDs grown at 0.15 ML/s, the wavelength shifts from 1.16 to 1.3 μm as the capping layer varies from GaAs to $In_{0.15}Ga_{0.85}As$. Further increase of indium fraction of InGaAs capping layer leads to further wavelength redshift as shown in Fig. 3. The same effect was observed for the quantum dot grown at the rate of 0.009 ML/s. For QDs grown at this rate, the longest GS transition wavelength of 1.4 μm with FE transition wavelength of 1.32 μm was achieved as the indium fraction in InGaAs capping layer reaches 0.3. More indium than 0.3 leads to a drastic decrease of PL intensity, which may be caused by dislocation formation. Since the FE provides a larger density of states (hence larger maximum gain), these QDs may be used as high gain material for 1.3 μm application.

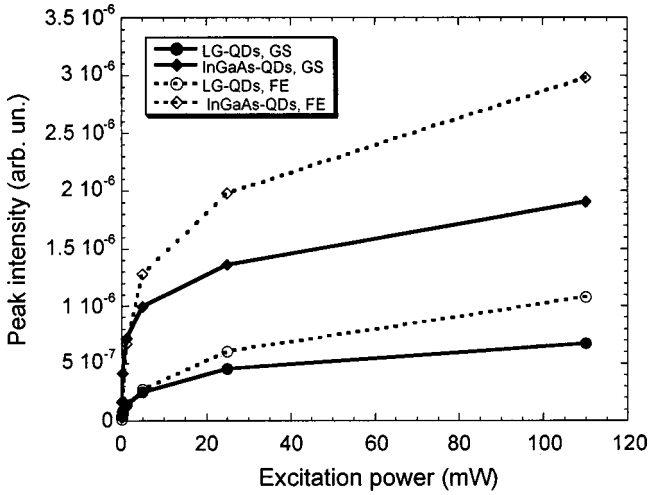

FIG. 4. Ground transition and first excited transition peak intensity of LG-QD and InGaAs-QD as a function of excitation power.

C. The comparison of optical properties of two kinds of QDs at 1.3 μm

Both approaches, quantum dots with extremely low growth (LG) rate of 0.009 ML/s and GaAs capping (shortened as LG-QDs hereafter) and QDs grown at 0.15 ML/s and capped with InGaAs (shortened as InGaAs-QDs hereafter), can provide the emission wavelength of 1.3 μm. It is very interesting to compare the radiative properties of the two kinds of dots. We performed excitation and temperature dependent PL measurements on both dots. The evolutions of the PL spectra (not shown here) at different excitation levels are similar. Only the ground and the first excited state transition were detectable at low excitation, while peaks corresponding to the second and the third excited state transition are observed at an excitation of 220 W/cm^2. The appearance of the excited states is due to the saturation of the ground state. Figure 4 shows ground and the first excited state transition peak intensity as the function of excitation power. As power increases, both the ground state and the first excited state of InGaAs-QDs increases much faster than that of LG-QDs. At excitation of 980 W/cm^2, the ground and the first excited state peak intensity of the InGaAs-QDs are 2.8 and 2.9 times higher, respectively, than those of the LG-QDs. The higher saturation level of the InGaAs-QD is the result of the higher areal density since the density of state is proportional to the areal density of quantum dots, which is consistent with our AFM measurements.

The line shape of the PL spectra of the two kinds of dots at different temperature are similar, as shown in Figs. 5(a) and 5(b). The ground state transitions dominate each spectrum while the two smaller peaks on the short wavelength side correspond to the first and second excited state transitions. With increasing temperature, the emission peaks shift toward longer wavelength, maintaining their shapes up to room temperature. The evolutions of the FWHM with temperature are also similar: 36 nm at 5 K and 47 nm at room temperature for LG-QDs, and 37 nm at 5 K and 45 nm at room temperature for InGaAs-QDs. At FWHM of less than 150 μeV have been reported for single QDs, the broadening

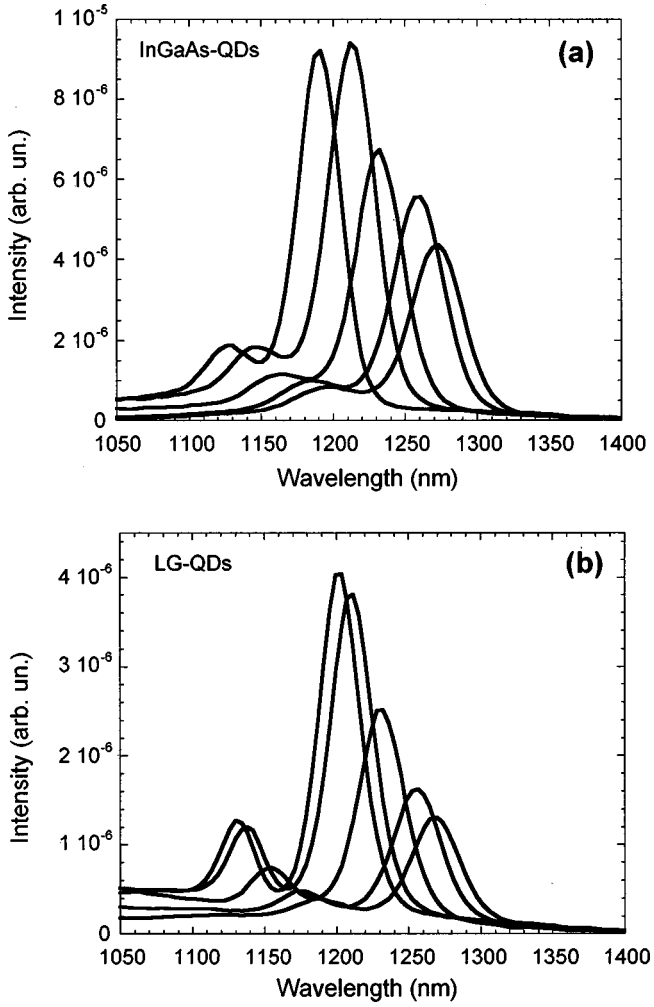

FIG. 5. PL spectra of InGaAs-QD (a) and LG-QD (b) at different temperatures.

at low temperature should be caused by dot size dispersion, while the linewidth increase at higher temperature is due to phonon-mediated homogeneous broadening.

The peak energy shift with increasing temperature, we found, can be described by the Varshni equation for semiconductor bulk material:

$$E_g = E_g(0) - \frac{\alpha T^2}{T+\beta}, \tag{1}$$

as shown in Fig. 6. The fitting parameters α, β are 4.58 $\times 10^{-4}$ eV/K, 243 K, and 4.54$\times 10^{-4}$ eV/K, 210 K for LG-QDs and InGaAs-QDs, respectively. A more detailed analysis reveals that the energy shifts of the ground state transition of the two kinds of QDs fall in between of that of the bulk InAs and GaAs band gaps. This shows that the energy shift with temperature is due to temperature dependent band gap shrinkage of QDs and WL layers.

Figure 7 displays the temperature dependence of the normalized integrated PL intensity of the ground state transition (the dominating transition in the PL spectra). The intensity remains constant with temperature up to 100 K for LG-QDs and 150 K for InGaAs-QDs. The intensity at room temperature drops a factor of 12 for LG-QDs compared to that of low

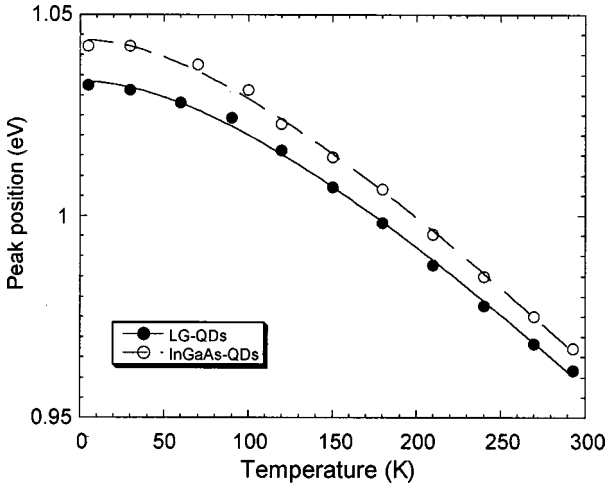

FIG. 6. PL peak energy of InGaAs-QD and LG-QD as a function of temperature.

temperature, and a factor of only 4 for InGaAs-QDs. The very small intensity decrease of a factor of 4 demonstrates the high quality of the InGaAs-QDs. The intensity evolution is fitted by assuming two thermally activated nonradiative recombination processes to compete with the radiative recombination:

$$I \propto \frac{1}{1+B_1 e^{-E_1/kT}+B_2 e^{-E_2/kT}}. \tag{2}$$

The relatively soft decrease at temperatures below 200 K corresponds to E_1 (105 and 71 meV for InGaAs-QDs and LG-QDs, respectively), and the steep decay above ~200 K corresponds to E_2 (285 and 345 meV for InGaAs-QDs and LG-QDs, respectively). Interestingly, these values are comparable to the values reported by Heitz *et al.*[19] for QDs grown with a different technique. The exact process is uncertain though there are several possibilities to explain the thermal quenching of PL intensity. One possible mechanism for E1 is the thermal escape of carrier from ground state to the excited states. If this is the case, E1 corresponds to the energy difference between the ground state and the first excited state, which is around 60 meV for two kinds of QDs. Another possibility for PL quenching is that the nonradiative transitions in the barrier compete with carrier capture and radiative transitions in the QDs. Then the E1 and E2 correspond to the thermal activation energy of the nonradiative center. It should be noted that the carrier capture process may slow down at elevated temperature, too.

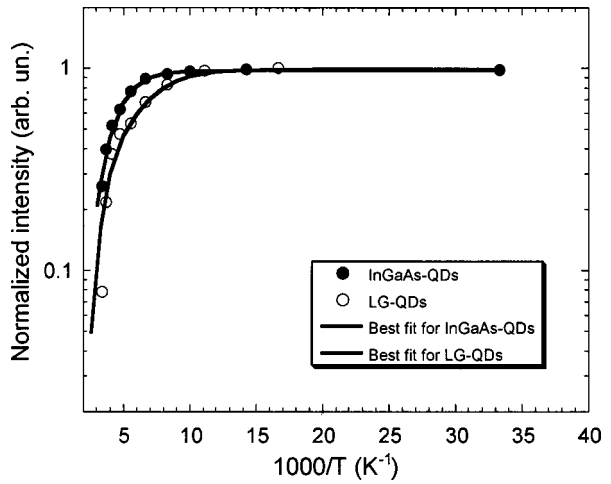

FIG. 7. Temperature dependence of the normalized integrated PL intensity of the ground state transition for InGaAs-QD and LG-QD.

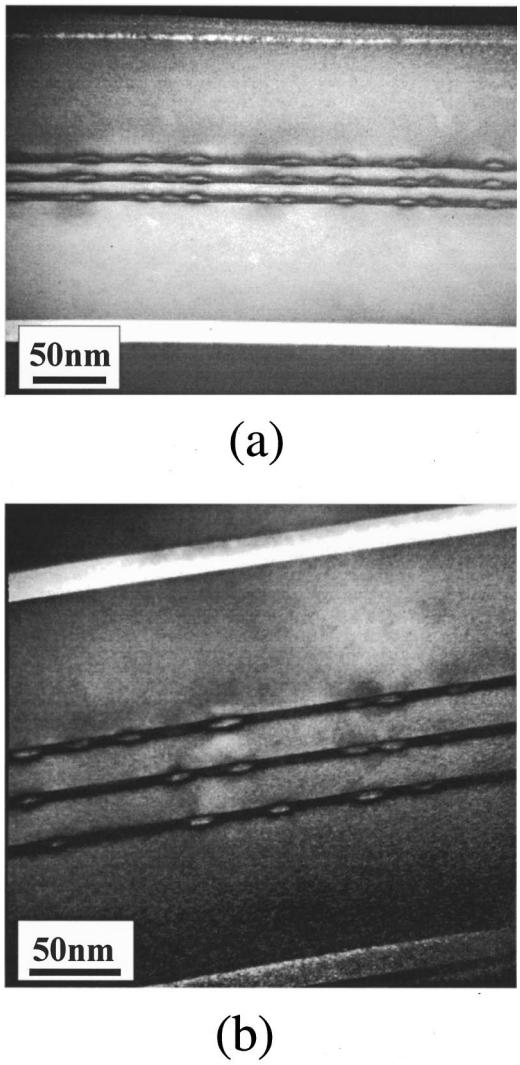

FIG. 8. [110] cross section dark-field ($g=200$) images of multiple QD layers grown with (a) 10 nm and (b) 25 nm thick spacers.

D. Stacking of the QDs

One important issue in QD structures is the gain saturation due to the finite number of states in the QD arrays. The gain saturation of the ground state transition will force QD structures to lase at higher state transitions resulting in higher thresholds. A simple method to over come gain saturation is to stack quantum dot layers. In our experiments, growth of three stacks of QD layers with different spacer thickness of 10 nm and 25 nm has been tested. Figure 8 shows the cross-sectional TEM images of samples. The stacked QDs with 10 nm spacer Fig. 8(a) are vertically correlated, while no clear vertical alignment is observed for QD stacks with 25 nm

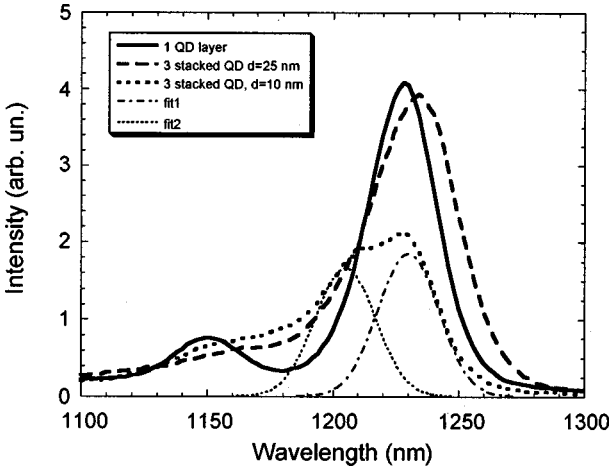

FIG. 9. PL spectra of one QD layer, three stacked QD layers with a 10 nm spacer and three stacks with 25 nm spacer QD layer.

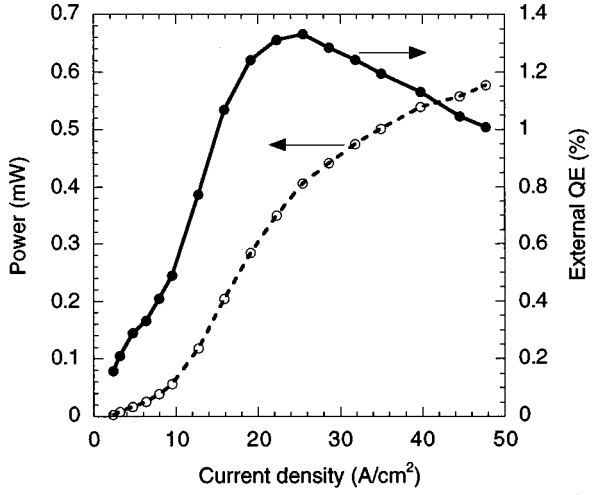

FIG. 10. The power output and the external QE as a function of injection current density.

spacer (b). The vertical alignment of the stacked QDs results in a dot size increase in the top layers, as shown in Fig. 8.

Figure 9 shows the 100 K PL spectra of one QD layer, three stacked QD layers with 10 and 25 nm spacing, respectively. The one QD layer and three stacked QD layers with a 25 nm spacer have similar spectra shape and intensity, while the intensity of three stacked QDs with a 10 nm spacer drops a factor of 2, with a broader spectrum. By fitting the spectrum, it is obvious that there are two groups of QD with different sizes, which is consistent with our TEM observation. The decrease in PL intensity of the three stacked QD layers with a 10 nm spacer indicates the deterioration of the structure.

E. Single mirror LEDs

An excellent method to measure the radiative efficiency of QDs is to fabricate light emitting diodes. In LED structures, spontaneous radiation is coupled out without amplification and therefore permits a direct evaluation of the radiative efficiency of the active layer. A LED at 1.3 μm itself is also very attractive for telecommunications due to its relatively simple epitaxial structure compared to a VCSEL. There are few reports on surface emitting diodes based on 1.3 μm InAs/GaAs QDs, and in most cases the reported efficiencies are much below those of InGaAs/GaAs quantum well structures (the typical radiative efficiency of InGaAs/GaAs quantum well at 1.0 μm is 80%–90%).

Bottom emitting single mirror light emitting diodes have been grown and processed. The whole epitaxial structures are as following: 0.6 μm *n*-GaAs buffer, 50 nm *n*-AlAs, 25 nm *n*-$Al_{0.5}Ga_{0.5}As$, 50 nm GaAs, active layer (InAs QDs $+In_{0.15}Ga_{0.85}As$), 50 nm GaAs, 25 nm *p*-$As_{0.5}Ga_{0.5}As$, 40 nm *p*-AlAs, and finally 142 nm *p*-GaAs. The InAs QDs were grown on a 2 nm $In_{0.15}Ga_{0.85}As$ surface (QDs on InGaAs). The insertion of 2 nm $In_{0.15}Ga_{0.85}As$ increases the dot areal density while not degrading the optical efficiency, as we have previously shown.[10] The SMLED is designed in such a way that the radiation emitted upwards and reflected by a broadband Au mirror constructively interferes with that emitted downwards, resulting in fourfold enhancement of light extraction from the bottom side. Devices with active area of 1.25×10^{-3} cm^2 were fabricated by wet etching and *p* (Au) and *n* (AuGeNi) contact evaporation. The top *p* contacts were not alloyed in order to keep a high reflectivity of the Au mirror.

Light–current measurements were performed under pulsed injection with 100 μs pulse width and 10% duty cycle. The light from the SMLED was collected and measured by a Ge detector via an integrating sphere. The electroluminescence output power is measured versus injection current while the external quantum efficiency (QE) is converted from the measured power by

$$\eta_{ex}=\frac{e}{h\nu}\frac{P_{out}}{I}, \tag{3}$$

where η_{ex} is the external quantum efficiency, P_{out} the power output, I the injection current, and ν the optical frequency. Figure 10 shows the power output and the external QE as a function of injection current density for the fabricated SMLEDs. The maximum external quantum efficiency is 1.3%. The external efficiency η_{ex} can be expressed as $\eta_{ex}=\eta_i\cdot\eta_{extr}$ (assuming 100% injection efficiency), where η_i and η_{extr} are internal radiative efficiency and extraction efficiency, respectively. The output coupling efficiency of the radiation was calculated using the simulation method based on the plane wave expansion of an electrical dipole emitter inside a multilayer structure.[20] The simulation gives an extraction efficiency of 6.2% after including the light absorption of the substrate. The radiative efficiency of the InAs QDs can then be deduced to be 21.5%. To our knowledge, a 21.5% radiative efficiency is the best one ever reported for active layers on GaAs at 1.3 μm. The high quantum efficiency of our samples is attributed to optimized growth of the QDs.

VI. CONCLUSION

In summary, we performed a systematic study of the effect of growth parameters on the structural and optical properties of InAs QDs grown under Stranski–Krastanov

mode. The dot density is significantly reduced as the growth rate decreases while the island size becomes larger. Meanwhile the emission wavelength shifts to longer side. By increasing the indium fraction in InGaAs capping layer, the emission wavelength increases accordingly. A ground state transition wavelength as long as 1.4 μm with excited state transition wavelength of around 1.3 μm has been obtained. The optical properties of QDs grown by different techniques have been compared. Finally SMLEDs with QDs embedded in InGaAs have been fabricated. The quantum efficiency at room temperature is 1.3%, corresponding to a radiative efficiency of 21.5%.

ACKNOWLEDGMENTS

This work is supported by the European project ''Gallium Arsenide Second Window Quantum Dot Lasers'' (GSQ) and by the Swiss National Science Foundation.

[1] Y. Arakawa and H. Sakaki, Appl. Phys. Lett. **40**, 939 (1982).
[2] M. Asada, Y. Miyamoto, and Y. Suematsu, IEEE J. Quantum Electron. **QE-22**, 1915 (1986).
[3] For a review, D. Bimberg, M. Grundmann, and N. N. Ledentsov, *Quantum Dot Heterostructures* (Wiley, Chichester, 1999).
[4] D. L. Huffaker, G. Park, Z. Zou, O. B. Shchekin, and D. G. Deppe, Appl. Phys. Lett. **73**, 2564 (1998).
[5] A. E. Zhukov *et al.*, IEEE Photonics Technol. Lett. **11**, 1345 (1999).
[6] Y. M. Shernyakov *et al.*, Electron. Lett. **35**, 898 (1999).
[7] G. T. Liu, A. Stintz, H. Li, T. C. Newell, A. L. Gray, P. M. Varangis, K. J. Malloy, and L. F. Lester, IEEE J. Quantum Electron. **36**, 1272 (2000).
[8] D. L. Huffaker and D. G. Deppe, Appl. Phys. Lett. **73**, 520 (1998).
[9] A. Fiore, U. Oesterle, R. P. Stanley, and M. Ilegems, IEEE Photonics Technol. Lett. **12**, 1601 (2000).
[10] J. X. Chen, U. Oesterle, A. Fiore, R. P. Stanley, M. Ilegems, and T. Todaro, Appl. Phys. Lett. **79**, 3681 (2001).
[11] H. Drexler, D. Leonard, W. Hansen, J. P. Kotthaus, and P. M. Petroff, Phys. Rev. Lett. **73**, 2252 (1994).
[12] P. Michler, A. Kiraz, C. Becher, W. V. Schoefeld, P. M. Petroff, L. Zhang, E. Hu, and A. Imamoglu, Nature (London) **290**, 2282 (2000).
[13] V. Zwiller, H. Blom, P. Jonsson, N. Paner, S. Jeppesin, T. Tsegaye, E. Goobar, M. Pisto, L. Samuelson, and G. Björk, Appl. Phys. Lett. **78**, 2476 (2001).
[14] M. V Maximov *et al.*, Physica E (Amsterdam) **7**, 326 (2000).
[15] N-T. Yeh, T.-E. Nee, J.-I. Chyi, T. M. Hsu, and C. C. Huang, Appl. Phys. Lett. **76**, 1567 (2000).
[16] P. B. Joyce, T. J. Krzyewski, G. R. Bell, and T. S. Jones, Phys. Rev. B **62**, 10 891 (2000).
[17] H. T. Dobbs, D. D. Vvedensky, A. Zangwill, J. Johansson, N. Carsson, and W. Seifert, Phys. Rev. Lett. **79**, 897 (1997).
[18] J. Tersoff, Phys. Rev. Lett. **81**, 3183 (1998).
[19] R. Heitz, I. Mukhametzhanov, A. Madhukar, A. Hoffmann, and D. Bimberg, J. Electron. Mater. **28**, 520 (1999).
[20] H. Benisty, R. P. Stanley, and M. Mayer, J. Opt. Soc. Am. A **15**, 1192 (1998).